

Gear Fault Diagnostics Using Extended Phase Space Topology

T. Haj Mohamad¹, and C. Nataraj²

^{1,2} Villanova Center for Analytics of Dynamical Systems (VCADS)
Villanova University, Villanova, PA 19085, USA
<http://www.vcads.org>

thajmoha@villanova.edu
nataraj@villanova.edu

ABSTRACT

This paper applies a novel feature extraction method called Extended Phase Space Topology (EPST) in order to diagnose various faults in a gear-train system. The EPST method, that our research team has been developing, is based on characterizing the vibration data using the topology of phase space, computing its density distribution and then expanded in a series of orthogonal functions. The resulting coefficients are subsequently used in a machine learning algorithm. For this study, multiple test gears with different health conditions (such as a healthy gear and defective gears with root crack on one tooth, multiple cracks on five teeth and missing tooth) are studied. The vibration data of a gear-train is measured by a triaxial accelerometer installed on the test. Results indicate that EPST is efficient in diagnosing the status of the health of the gear system and characterizing the dynamic behavior. Moreover, the EPST procedure does not require *a priori* knowledge about the dynamics of the system. EPST needs no noise reduction, signal preprocessing, feature ranking or selection, and therefore can easily be applied in a relatively automated process.

1. INTRODUCTION

Machine condition monitoring techniques have received much attention in recent years due to their significant advantages in increasing productivity and lifespan of system components. Moreover, condition monitoring techniques decrease maintenance costs, which comprise a major part of operating costs in any industry. Gears are essential elements in most rotating machines and play a critical role as transmission systems. A considerable number of studies have focused on condition monitoring of gears because of the complex

nonlinearity of faults in gears which makes abnormality diagnostics difficult (Randall, 1982; Chad, 1998; Jardine, Lin, & Banjevic, 2006; Serridge, 1990). Vibration and acoustic methods contain valuable information about the condition of the rotating machines such as gears, and therefore, they are the most widely used for fault diagnostics of gears (Bajric, Zuber, & Isic, 2013; Hussain & A.Gabbar, 2011; W. Q. Wang, Ismail, & Farid Golnaraghi, 2001; Dalpiaz, Rivola, & Rubini, 2000).

One of the techniques most commonly applied to machine fault detection problems is the pattern recognition approach. The pattern recognition approach, which involves classification model techniques, uses data collected from dynamical systems to extract a feature set, known as a condition indicator or condition signature, in order to detect and identify the system's current state of health (Bishop, 2006; Vachtsevanos, Lewis, Roemer, Hess, & Wu, 2006). The objective of feature extraction is to characterize the system response in an unmatched way and to acquire accurate diagnostic information about the system. These features should be informative and non-redundant.

Various feature extraction techniques have studied gear fault detection and diagnostics (W. J. Wang & McFadden, 1996; Peng & Chu, 2004; Combet & Gelman, 2007; Hussain & A.Gabbar, 2011; Yuan, He, & Zi, 2010; Mohammed, Rantatalo, Aidanp, & Kumar, 2013; Li, Zhang, & Wu, 2017; Mohammed & Rantatalo, 2016; Hong et al., 2017). These feature extraction techniques can be categorized into time domain, frequency domain, and time-frequency domain techniques. Each of these techniques has its own limitations and strengths. In frequency domain techniques, analysis of the sideband frequencies in the frequency spectrum indicate faults in the gearbox but do not necessarily distinguish gear faults as they may be located in other components of the gearbox (Randall, 2011; Peng, Yu, & Luo, 2011). Studies in (Syta, Jonak, Jedlinski, & Litak, 2012) show that frequency analysis is not effective in differentiating between

Turki Haj Mohamad et al. This is an open-access article distributed under the terms of the Creative Commons Attribution 3.0 United States License, which permits unrestricted use, distribution, and reproduction in any medium, provided the original author and source are credited.

healthy gears and defective gears with a single crack. On the other hand, time domain techniques such as Time Synchronous Averaging (TSA) were found to hardly distinguish between different faults, particularly in the early stage of the fault or in the case of multiple simultaneous faults in different gears (Salem, 2012; Kwiimy, Kankar, Chen, Chaudhry, & Nataraj, 2015). Furthermore, the TSA technique requires too much time and is computationally intensive which makes it inconvenient for online detection (Vachtsevanos et al., 2006). These limitations motivate the need for a robust and reliable method for gear fault detection and diagnostics.

In earlier work, we introduced the Phase Space Topology (PST) method to describe and distinguish the topology of the phase space trajectory with quantitative measures. (Samadani, Kwiimy, & Nataraj, 2015, 2013). The PST was applied to a variety of nonlinear systems ranging from a magnetically actuated pendulum system to a six degree-of-freedom nonlinear oscillator in order to estimate the parameters of each system and to characterize different conditions of each system. As an extension of the previous work, the Extended Phase Space Topology (EPST) was introduced in (Samadani, Haj Mohamad, & Nataraj, 2016; Haj Mohamad, Kwiimy, & Nataraj, 2017) as a machinery diagnostics method. The EPST is based on the quantitative characterization of the topology of the density distribution of the vibration signal. The method was applied to a rotor-bearing system in order to detect and diagnose various bearing conditions. The results showed that EPST performed significantly better compared with traditional statistical feature methods. In general, feature extraction is an application-dependent process, however, in this paper we are expanding the previous work by generalizing the applicability of the method by applying it to another dynamic application. As we will show, the EPST can be implemented in various dynamical systems with minimal expert knowledge about the nature of the problem.

The proposed method has been applied to vibration data of a helicopter gearbox mock-up system (5 m long). For this study, multiple test gears with different health conditions (such as healthy gears and defective gears with root crack on one tooth, multiple cracks on five teeth and missing tooth) are studied. The vibrational signals were recorded using a triaxial accelerometer installed on the test gearbox.

The rest of this paper is organized as follows. In Section 2, the mathematical details of the EPST are introduced. Section 3 represents the experimental setup of the gear-train and measurement of data. Section 4 discusses the analysis process of the density distribution, and the classification model results. Finally, Section 5 summarizes and concludes the paper.

2. EXTENDED PHASE SPACE TOPOLOGY METHOD

Let $X=(x_1, x_2, \dots, x_n)$ be an independent and identically distributed sampled data drawn from a distribution with an un-

known density function f . The shape of this function can be estimated by its kernel density estimator. Kernel density estimators are the most widely used in the class of nonparametric probability density estimation methods. The kernel estimator is defined as:

$$\hat{f}_h(x) = \frac{1}{nh} \sum_{i=1}^n K\left(\frac{x-x_i}{h}\right) \quad (1)$$

The $\hat{\cdot}$ symbol indicates that the density distribution is an estimate, and h indicates that its value can depend on h . $K(\cdot)$ is the kernel function which is typically a symmetric probability density function with finite variance. A kernel function of probability mass n^{-1} is placed at each data point and the summation of these kernel functions will produce the estimated density distribution. The kernel function satisfies the following requirements:

$$\int_{-\infty}^{\infty} K(u)du = 1 \quad (2)$$

$$K(-u) = K(u) \quad \forall u \quad (3)$$

There is a range of kernel functions that can be used, including uniform, triangular, biweight, triweight, Epanechnikov, normal, etc. Due to its conventional and convenient mathematical properties, we use the standard normal density function in our approach, defined as the following:

$$K(u) = \frac{1}{\sqrt{2\pi}} e^{-\frac{1}{2}u^2} \quad (4)$$

The performance of the kernel density estimator depends mainly on the smoothing parameter h . For normal kernel functions, the optimal choice for the bandwidth based on Silverman's rule of thumb is as follows:

$$h = \left(\frac{4\hat{\sigma}^5}{3n}\right)^{\frac{1}{5}} \quad (5)$$

where, $\hat{\sigma}$ is the standard deviation of the samples and n is the number of sampled data. Let x be a state of the system and $y_d = \hat{f}_h(x)$, its density computed using Kernel density estimator. y_d is then approximated with Legendre orthogonal polynomials. Legendre polynomials can directly be obtained from Rodrigues' formula which is given by

$$P_m(x) = \frac{1}{2^m m!} \frac{d^m}{dx^m} [(x^2 - 1)^m] \quad (6)$$

where, $m = 0, 1, 2, \dots$ or can be obtained from the recursive definition using Bonnet's recursion formula given by

$$(m+1)P_{m+1}(x) = (2m+1)xP_m(x) - mP_{m-1}(x) \quad (7)$$

where, the first two terms are given by

$$P_0(x) = 1, \quad P_1(x) = x \quad (8)$$

The coefficients of the Legendre polynomials are obtained by using the linear least squares method assuming the following linear regression model.

$$f(x, \beta) = \sum_{j=1}^m \beta_j P_j(x) \quad (9)$$

Letting

$$X_{ij} = \frac{\partial f(x_i, \beta)}{\partial \beta_j} = P_j(x_i) \quad (10)$$

The estimated coefficients are given by

$$\hat{\beta} = (X^T X)^{-1} X^T y_d \quad (11)$$

The coefficients, $\hat{\beta}$ are the features in our approach that can be used in classification or regression problems.

Using Legendre Polynomials and the computed coefficients, we can approximate the density as the following.

$$f = X \hat{\beta} \quad (12)$$

In order to measure the quality of the fit, two measures including Root Mean Square Error (RMSE) and Pearson's Correlation Coefficient (PCC) are used which are defined as the following:

$$RMSE = \sqrt{\frac{1}{N} Z Z^T} \quad (13)$$

where $Z = y_d - f$ is the residual and N is the number of points in the density function.

$$PCC = \frac{a^T b}{\sqrt{(a^T a)(b^T b)}} \quad (14)$$

where $a = y_d - E\{y_d\}$ and $b = f - E\{f\}$, $E\{\cdot\}$ is the expected value.

3. EXPERIMENTAL SETUP AND DATA COLLECTION

The gear-train experimental set up, which is a mock-up of a helicopter gear box system, is located at the United Technologies Research Center (UTRC). The gear-train (shown in Fig.1) is a large scale machine (5 m long) consisting of a motor, dynamometer and four gearboxes, where each gearbox contains four spur gears. The schematic of the gear-train illustrating the four gear boxes and their components is shown in Fig.2. For this study, multiple test gears with different health conditions were studied. The study was implemented by replacing the gear located in gearbox number 3 and shown in green color in Fig.2 with different test gears while the remaining setup components were kept unchanged. The test gears with 23 teeth that were used in the experiment include one healthy gear and three defective gears with root crack on one tooth, multiple cracks on five teeth and missing tooth. Fig. 3 illustrates the various gear defects: a) shows the single root crack of 2 mm b) shows the locations of the five root



Figure 1. Gear-train experimental setup

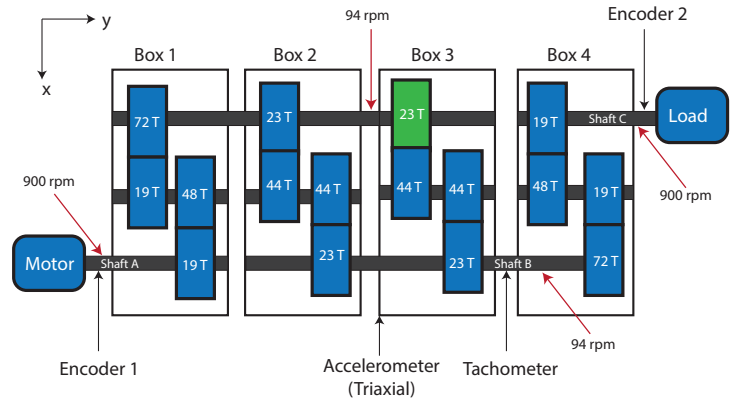


Figure 2. Gear-train schematic

cracks on teeth numbers 1,6,10,15, and 19 c) shows the sizes of the five root cracks ranging from 0.5 mm to 2.5 mm.

The vibrational signals were recorded using a triaxial accelerometer installed on gearbox number 3. The vibrational data was measured at the sampling frequency of 102,400 Hz. The rotational speeds of shafts A, C, and B were measured using two encoders and a tachometer. Two encoders were installed at shaft "A" and shaft "C" to measure their rotational speeds with a 360 pulse/rev resolution. The tachometer on shaft "B" was used to measure the shaft rotational speed at a rate of 1 pulse/rev. Due to the gear teeth ratio, the test gear shaft operates at the same speed as shaft "B". In this study, the motor was operating at a rotational speed of 900 rpm while the test gear shaft was running at 94 rpm for the different gear conditions. The vibrational signals of gearbox number 3 were recorded for 64 seconds for healthy, single crack tooth and multiple crack teeth conditions, and for 3.2 seconds for the missing tooth condition. Samples of the measured vibra-

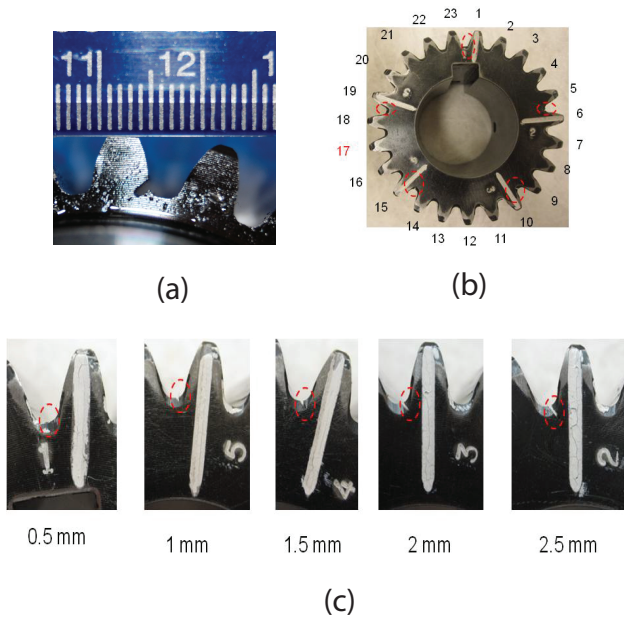


Figure 3. Gear defects: a) crack on one tooth b) crack on 5 teeth c) crack sizes on 5 teeth.

tion for different gear conditions in the three directions are shown in Fig. 4.

4. ANALYSIS AND FAULT CLASSIFICATION

In order to analyze the vibration data measured by the accelerometer for various gear conditions, vibration data was divided into multiple segments of revolutions using the tachometer signal which provides the shaft phase information. The segment $x_k(i)$, for $i = 1, 2, \dots, N$ is the vibration data of revolution k of a total number of K revolutions. The total number of data segments that were obtained is 1,011 segments in x, y and z directions. In each direction, 97 data segments were obtained for each healthy, single crack defect, and multiple crack defect conditions while 46 data segments were obtained for the missing tooth defect condition. The density distribution of the vibration data is estimated using kernel density estimation method. Samples of the estimated density distributions for different gear conditions in x, y and z directions are shown in Figures 5, 6, and 7, respectively.

First, the density distributions in the x direction are analyzed. By comparing the density distribution of the vibration data in the x direction for the four gear conditions, one finds that the healthy condition is easily distinguished from the other gear conditions. The estimated density for the healthy condition has two different modes, the most frequently occurring states, which appear as two distinct peaks. On the other hand, the estimated density of the multiple crack and the missing tooth conditions have a symmetric unimodal distri-

bution. Both density distributions have a single peak around zero. The missing tooth condition, in contrast to the multiple crack condition, has a smaller standard deviation and a higher peak amplitude. The estimated density of the single crack condition has a bimodal distribution with a narrower distribution range compared to the healthy condition.

Second, analyzing the density distributions in y direction, figure 6 shows that the density of the multiple crack condition has a left, or negative, skewed distribution while the density of the missing tooth condition has a high single peak with a mean of zero. The density of the single crack condition in the y direction has a similar distribution to the x direction but with a higher amplitude.

Finally, densities of the vibration data in the z direction are shown fig 7. The estimated densities of the healthy and single crack condition approximately look the same. The density distribution of the multiple crack condition seems to have two modes (bimodal distribution). These observations indicate that the density distribution of the vibration data provides valuable information for characterizing the dynamic response of different gear conditions. This observation suggests the implementation of the density distribution for fault detection and identification in gears.

The EPST method, which is based on characterizing the topology of the density distribution of the vibration data, is applied by mapping the data onto a density space for each condition and then approximating these densities using Legendre polynomials. Fig 8 illustrates the process of the EPST method. After the density plots were estimated, the plots were then approximated using Legendre polynomials of order 30. The order was selected based on the best fit between the actual and the approximate densities by calculating the root mean square error (RMSE) and Pearson's Correlation Coefficient (PCC). Figure 9 shows the actual estimated density (black) and its approximation (blue) for the healthy gear conditions in the x direction. The figure also shows the values of RMSE and PCC with 0.0217 and 1.0 respectively.

The coefficients of Legendre polynomials were used as features to represent each gear condition for inputs to an artificial neural network (ANN). For every gear condition, the first 10 coefficients in each direction were considered as a feature vector, making 30 features in total. A neural network of 10 hidden neurons was trained using 50% of the data samples (168 cases) and backpropagation algorithm. Additionally, 15% (52 cases) of the data samples were used for validating the trained classifier and the remaining 35% (117 cases) of the data samples were used for testing the classifier.

The effectiveness of the classification model for the training and testing data is presented by means of confusion matrix plots. The confusion matrix of the classification model for training and test data are shown in Fig.10. In the confusion

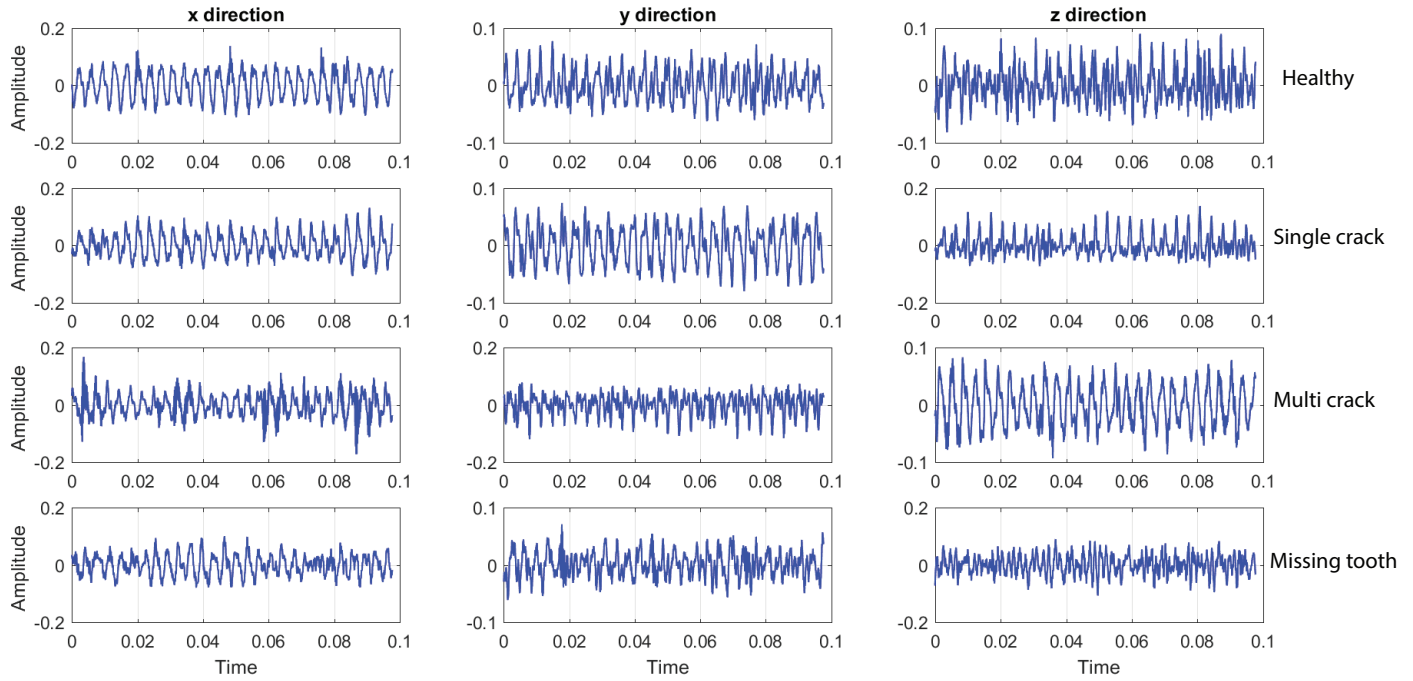


Figure 4. Samples of the gear vibration data for each configuration and direction

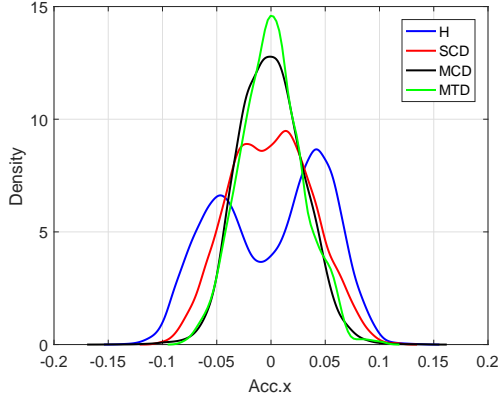


Figure 5. Density distribution of vibration in x direction

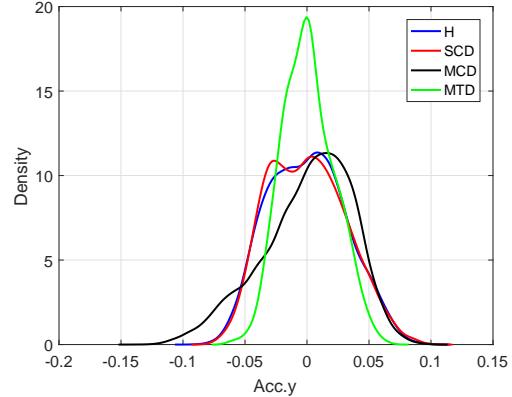


Figure 6. Density distribution of vibration in y direction

matrix, the diagonal cells show the number and percentage of correct classifications by the trained classifier while the off diagonal cells represent the misclassified predictions.

The training confusion matrix shows virtually perfect results where all predictions are on the diagonal. In the test confusion matrix, 117 cases with different gear conditions were used to test the trained classification model. 31 cases were correctly classified as healthy condition. This corresponds to 26.3% of all 117 cases. Similarly, 38 cases were correctly classified as single crack defect condition. This corresponds

to 32.2% of all cases. Furthermore, one of the missing tooth defect cases was incorrectly classified as healthy condition and this corresponds to 0.8% of all 117 cases under study. Healthy condition is designated as negative class and defective condition is designated as positive class. True positive (TP) is correctly classified for each defective condition, false positive (FP) is incorrectly classified for each defective condition. It is important to note that misclassification between defective conditions is also counted. In contrast, true negative (TN) is correctly classified as healthy condition and false negative (FN) is incorrectly classified as healthy condition. For

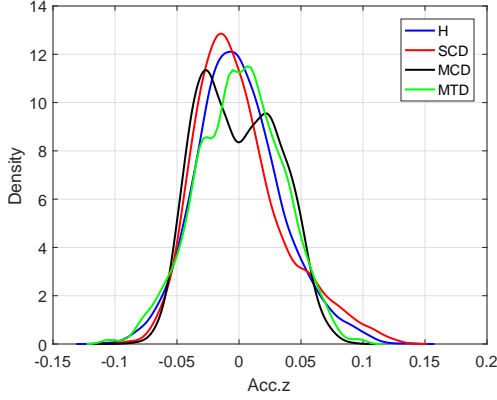


Figure 7. Density distribution of vibration in z direction

example in the test confusion matrix (figure 10) $TN = 31$, $TP = 86$, $FN = 1$, and $FP = 0$.

To describe the performance of the confusion matrices in a simpler way, evaluating matrices such as overall accuracy, F1 score, sensitivity and precision are calculated from the confusion matrices. Below is a description of the performance rates used to evaluate the classifier.

Accuracy is the rate of the correct prediction

$$ACC = \frac{TP + TN}{TP + FP + TN + FN} \quad (15)$$

The best accuracy is 1.0 while the worst is zero. Sensitivity, which is also known as recall or true positive rate, is

$$SEN = \frac{TP}{TP + FN} \quad (16)$$

The best sensitivity is 1.0 and the worst is zero. Precision is the correct positive prediction divided by the total number of positive predictions:

$$PREC = \frac{TP}{TP + FP} \quad (17)$$

Finally, F-score is the harmonic mean of sensitivity and precision:

$$F_{\beta} = \frac{(1 + \beta^2)(PREC \times SEN)}{\beta^2(PREC + SEN)} \quad (18)$$

where, β is a constant that could be 0.5, 1, 2 depending on the F-score used. In this study, F_1 score was used for evaluating the performance where sensitivity and precision are evenly weighted.

Table 1 shows the performance of the training and the test confusion matrices. The results indicate 100% overall accuracy, F1 score, sensitivity and precision for the training classifier. Furthermore, the results indicate 99.2% overall accuracy and 99% F1 score for the test classifier with only one misclas-

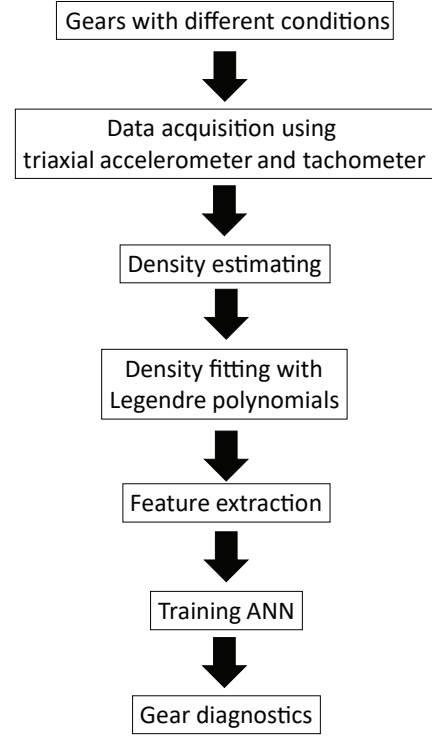


Figure 8. The process of the EPST

sification. The sensitivity of the classifier in predicting healthy, single crack and multiple crack conditions is 1.0, while it is 0.95 for the missing tooth condition due to one misclassification. On the other hand, the precision of the classifier for all gear defects is 1.0 and 0.97 for healthy condition due to a misclassified missing tooth condition as a healthy condition.

5. CONCLUSION

In this paper, a mock-up of a helicopter gear box system is studied in order to detect and identify different gear faults. Four gear conditions including healthy, single crack, multiple crack, and missing tooth were investigated under one operating condition. The EPST method, which is based on characterizing the topology of the density distribution of the vibration data, was applied. The density distribution of the vibration signal was approximated using Legendre polynomials. Then, the coefficients of the orthogonal polynomials were used as features in an artificial neural network to distinguish between the different gear conditions in the study.

Our results show that the density distribution provides rich information regarding the gear status. Furthermore, the results showed that the EPST has an outstanding performance in gear fault detection and identification with minimal knowl-

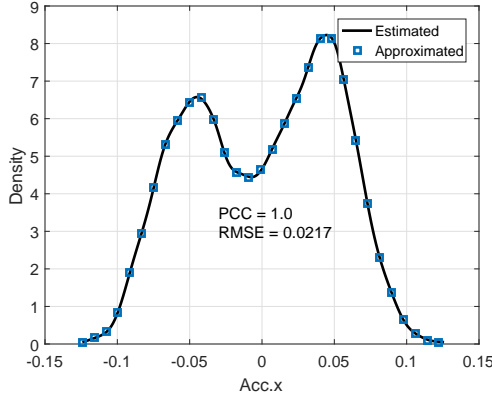


Figure 9. Density fitting using Legendre polynomials

Table 1. Performance measures

Training classifier evaluation				
Condition	Sensitivity	Precision	Overall	
Healthy	1.0	1.0	Accuracy	F1
Single Crack	1.0	1.0		
Multi Crack	1.0	1.0	1.0	1.0
Missing Tooth	1.0	1.0		
Test classifier evaluation				
Condition	Sensitivity	Precision	Overall	
Healthy	1.0	0.97	Accuracy	F1
Single Crack	1.0	1		
Multi Crack	1.0	1	0.99	0.99
Missing Tooth	0.95	1		

edge about the dynamic response of the system. Finally, the current study was performed on a single operation condition (10 hp load and 900 rpm speed motor); thus, future work will investigate the gear-train under variable operating conditions.

ACKNOWLEDGMENTS

This work is supported by the US Office of Naval Research under the grant ONR N00014-15-1-2311 with Capt. Lynn Petersen as the Program Manager. We deeply appreciate this support and are humbled by ONR’s enthusiastic recognition of the importance of this research. We are also grateful to United Technologies Research Center for providing the test data; in particular, we would like to acknowledge the willing help provided by Dr. Zaffir Chaudhry and Dr. Yan Chen.

Training Confusion Matrix

		Actual			
		H	SCD	MCD	MTD
Predicted	H	51 30.4%	0 0.0%	0 0.0%	0 0.0%
	SCD	0 0.0%	46 27.4%	0 0.0%	0 0.0%
	MCD	0 0.0%	0 0.0%	46 27.4%	0 0.0%
	MTD	0 0.0%	0 0.0%	0 0.0%	25 14.9%

Test Confusion Matrix

		Actual			
		H	SCD	MCD	MTD
Predicted	H	31 26.3%	0 0.0%	0 0.0%	1 0.8%
	SCD	0 0.0%	38 32.2%	0 0.0%	0 0.0%
	MCD	0 0.0%	0 0.0%	30 25.4%	0 0.0%
	MTD	0 0.0%	0 0.0%	0 0.0%	18 15.3%

Figure 10. Training and testing confusion matrices

NOMENCLATURE

- f unknown density function
- \hat{f} estimated density function
- y_d computed estimated density
- h bandwidth
- $K(\cdot)$ kernel function
- n number of data points
- u dummy variable
- $\hat{\sigma}$ estimated standard deviation
- P_m the m th Legendre polynomial
- β Legendre polynomials coefficients
- $\hat{\beta}$ estimated Legendre polynomials coefficients
- $RMSE$ Root Mean Square Error
- Z residual
- N number of estimated density points
- PCC Pearson’s Correlation Coefficient
- a, b residual

REFERENCES

- Bajric, R., Zuber, N., & Isic, S. (2013, 09). Recent advances in vibration signal processing techniques for gear fault detection-A review. *Applied Mechanics and Materials*, 430, 78-83.
- Bishop, C. (2006). *Pattern recognition and machine learning*. Springer-Verlag, New York.
- Chad, E. F. (1998). *Synchronous sampling sideband orders from helical planetary gear sets* (Unpublished master's thesis). Blacksburg, Virginia,.
- Combet, F., & Gelman, L. (2007). An automated methodology for performing time synchronous averaging of a gearbox signal without speed sensor. *Mechanical Systems and Signal Processing*, 21(6), 2590 - 2606. doi: {<https://doi.org/10.1016/j.ymssp.2006.12.006>}
- Dalpiaz, G., Rivola, A., & Rubini, R. (2000, May). Effectiveness and Sensitivity of Vibration Processing Techniques for Local Fault Detection in Gears. *Mechanical Systems and Signal Processing*, 14, 387-412. doi: 10.1006/mssp.1999.1294
- Haj Mohamad, T., Kwuimy, C. K., & Nataraj, C. (2017). Discrimination of Multiple Faults in Bearings Using Density-Based Orthogonal Functions of the Time Response. *International Design Engineering Technical Conferences and Computers and Information in Engineering Conference*.
- Hong, L., Qu, Y., Dhupia, J. S., Sheng, S., Tan, Y., & Zhou, Z. (2017). A novel vibration-based fault diagnostic algorithm for gearboxes under speed fluctuations without rotational speed measurement. *Mechanical Systems and Signal Processing*, 94, 14 - 32. doi: <https://doi.org/10.1016/j.ymssp.2017.02.024>
- Hussain, S., & A.Gabbar, H. (2011, 05). A novel method for real time gear fault detection based on pulse shape analysis. *Mechanical Systems and Signal Processing*, 25, 1287-1298.
- Jardine, A. K. S., Lin, D., & Banjevic, D. (2006, October). A review on machinery diagnostics and prognostics implementing condition-based maintenance. *Mechanical Systems and Signal Processing*, 20, 1483-1510. doi: 10.1016/j.ymssp.2005.09.012
- Kwuimy, C. A. K., Kankar, P. K., Chen, Y., Chaudhry, Z., & Nataraj, C. (2015). Development of Recurrence Analysis for Fault Discrimination in Gears. *International Design Engineering Technical Conferences and Computers and Information in Engineering Conference, Volume 8: 27th Conference on Mechanical Vibration and Noise*.
- Li, B., Zhang, X., & Wu, J. (2017). New procedure for gear fault detection and diagnosis using instantaneous angular speed. *Mechanical Systems and Signal Processing*, 85, 415 - 428. doi: <https://doi.org/10.1016/j.ymssp.2016.08.036>
- Mohammed, O. D., & Rantatalo, M. (2016). Dynamic response and time-frequency analysis for gear tooth crack detection. *Mechanical Systems and Signal Processing*, 6667, 612 - 624. doi: <https://doi.org/10.1016/j.ymssp.2015.05.015>
- Mohammed, O. D., Rantatalo, M., Aidanp, J.-O., & Kumar, U. (2013). Vibration signal analysis for gear fault diagnosis with various crack progression scenarios. *Mechanical Systems and Signal Processing*, 41(12), 176 - 195. doi: <https://doi.org/10.1016/j.ymssp.2013.06.040>
- Peng, F., Yu, D., & Luo, J. (2011). Sparse signal decomposition method based on multi-scale chirplet and its application to the fault diagnosis of gearboxes. *Mechanical Systems and Signal Processing*, 25(2), 549 - 557.
- Peng, Z., & Chu, F. (2004, February). Application of the wavelet transform in machine condition monitoring and fault diagnostics: a review with bibliography. *Mech. Syst. Signal Process.*, 18, 1992-21. doi: 10.1016/S0888-3270(03)00075-X
- Randall, R. B. (1982). A new method of modelling gear faults. *ASME Journal of Mechanical Design*, 104(2), 259-267.
- Randall, R. B. (2011). *Vibration-based condition monitoring*. John Wiley & Sons, Ltd.
- Salem, A.-A. (2012). *Condition monitoring of gear systems using vibration analysis* (Unpublished doctoral dissertation). University of Huddersfield.
- Samadani, M., Haj Mohamad, T., & Nataraj, C. (2016). Feature Extraction for Bearing Diagnostics Based on the Characterization of Orbit Plots With Orthogonal Functions. *International Design Engineering Technical Conferences and Computers and Information in Engineering Conference, Volume 8: 28th Conference on Mechanical Vibration and Noise*.
- Samadani, M., Kwuimy, C. K., & Nataraj, C. (2013). Diagnostics of a nonlinear pendulum using computational intelligence. In *Asme 2013 dynamic systems and control conference*.
- Samadani, M., Kwuimy, C. K., & Nataraj, C. (2015). Model-based fault diagnostics of nonlinear systems using the features of the phase space response. *Communications in Nonlinear Science and Numerical Simulation*, 20(2), 583-593.
- Serridge, M. (1990). Ten crucial concepts behind trustworthy fault detection in machine condition monitoring. In J. M. Montalvão e Silva & F. A. Pina da Silva (Eds.), *Vibration and wear in high speed rotating machinery* (pp. 729-740). Dordrecht: Springer Netherlands.
- Syta, A., Jonak, J., Jedlinski, L., & Litak, G. (2012). Failure diagnosis of a gear box by recurrences. *Journal of Vibration and Acoustics*, 134, 041006.
- Vachtsevanos, G., Lewis, F., Roemer, M., Hess, A., & Wu, B. (Eds.). (2006). *Intelligent fault diagnosis and prognos-*

sis for engineering systems. Wiley.

Wang, W. J., & McFadden, P. D. (1996, May). Application of Wavelets to Gearbox Vibration Signals for Fault Detection. *Journal of Sound Vibration*, *192*, 927-939. doi: 10.1006/jsvi.1996.0226

Wang, W. Q., Ismail, F., & Farid Golnaraghi, M. (2001, September). Assessment of Gear Damage Monitoring Techniques Using Vibration Measurements. *Mechani-*

cal Systems and Signal Processing, *15*, 905-922. doi: 10.1006/mssp.2001.1392

Yuan, J., He, Z., & Zi, Y. (2010). Gear fault detection using customized multiwavelet lifting schemes. *Mechanical Systems and Signal Processing*, *24*(5), 1509 - 1528. (Special Issue: Operational Modal Analysis) doi: <https://doi.org/10.1016/j.ymsp.2009.11.003>